

# Nanometer-Sized Electrochemical Sensors

Yuanhua Shao and Michael V. Mirkin\*

Department of Chemistry and Biochemistry, Queens College—CUNY, Flushing, New York 11367

Galina Fish, Sofia Kokotov, Daniel Palanker, and Aaron Lewis

School of Applied Sciences and Technology, The Hebrew University of Jerusalem, Jerusalem, Israel 91904

**Nanometer-sized glass-sealed metal ultramicroelectrodes (UMEs) have been prepared using a laser-based micropipet puller. The tip was exposed to solution either by etching away a small portion of glass insulator or by micropolishing. The characterization of the UMEs was carried out by a combination of steady-state voltammetry, scanning electron microscopy (SEM), and scanning electrochemical microscopy (SECM). The cyclic voltammograms obtained have a regular shape with very small capacitive and resistive background. The effective electrode radii obtained from voltammetry were between 2 and 500 nm. From the SEM micrographs, the shape of polished tips appears to be close to a microdisk, while the geometry of etched electrodes is closer to conical. Accordingly, the SECM current–distance curves ( $i_T$ – $d$ ) obtained with polished electrodes fit well the theory for a disk-shaped tip, while a 20-nm-radius etched electrode was shown to be a fairly sharp cone with a height-to-radius ratio of about 2.5. The experimental data were compared to the theory developed for disk-shaped, conical, and recessed tips to demonstrate suitability of the produced electrodes for quantitative electrochemical experiments. The prospects of steady-state measurements of the rates of fast heterogeneous reactions are discussed. Submicrometer-sized ion selective electrodes (ISEs) were prepared by coating etched Ag tips with silver iodide. The concentration response of such ISEs remained stable and linear after coating of the ISEs with protective Nafion film.**

The introduction of micrometer-sized electrodes led to significant advances in studies of fast heterogeneous and homogeneous reactions, measurements in various microenvironments, and high-resolution electrochemical imaging.<sup>1</sup> Even smaller, i.e., nanometer-sized, ultramicroelectrodes (UMEs) are required for characterization of the electrode/electrolyte interfacial processes with nanometer-scale resolution.<sup>2</sup> The initial stages of many important processes, such as metal corrosion and heterogeneous nucleation, include formation of nanometer-sized transient structures.<sup>3</sup> To probe such structures electrochemically, one needs a comparably

sized electrode. Another important application of ultrasmall electrodes is single-molecule detection.<sup>4</sup> During the last several years, a few research groups have been exploring different methodologies of manufacturing nanometer-sized disks, bands, cones, and arrays of UMEs.<sup>5–10</sup> The main difficulty in using such electrodes for quantitative measurements is the shape uncertainty. In this paper, we develop procedures for easier preparation and better characterization of nanometer-sized electrochemical sensors.

The voltammetric response of an UME does not provide sufficient information about the geometry of either the conductor exposed to electrolyte or the insulating sheath. The diffusion to a small electrode (hemisphere, cone, disk) rapidly becomes hemispherical when the electrode is in the bulk solution far from any object.<sup>11</sup> Thus, the shape of a reversible steady-state voltammogram is the same for any microelectrode geometry. In contrast, an irregularly shaped UME employed in kinetic measurements may result in highly erroneous values for rate constants extracted from experimental data.<sup>12</sup>

Figure 1 presents several electrode shapes that can result from different preparation procedures. A perfect microdisk UME (Figure 1A) is very unlikely to be produced when the radius,  $a$ , is less than about 2  $\mu\text{m}$ . Instead, one can make an irregularly shaped planar electrode (Figure 1B), whose effective radius can be calculated from the diffusion-limiting steady-state current assuming disk geometry:

$$i_{T,\infty} = 4nFDc^\circ a \quad (1)$$

where  $c^\circ$  is the bulk concentration of the mediator species,  $D$  is the diffusion coefficient,  $F$  is the Faraday constant, and  $n$  is the number of electrons transferred. Such electrodes have commonly been employed in both steady-state and non-steady-state measure-

- (1) (a) Wightman, R. M.; Wipf, D. O. In *Electroanalytical Chemistry*; Bard, A. J., Ed.; Marcel Dekker: New York, 1989; Vol. 15, p 267. (b) Forster, R. J. *Chem. Soc. Rev.* **1994**, 289. (c) Amatore, C. In *Physical Electrochemistry: Principles, Methods, and Applications*; Rubinstein, I., Ed.; Marcel Dekker: New York, 1995; p 131.
- (2) Bard, A. J.; Abruña, H. D.; Chidsey, C. E.; Faulkner, L. R.; Feldberg, S. W.; Itaya, K.; Majda, M.; Melroy, O.; Murray, R. W.; Porter, M. D.; Soriaga, M. P.; White H. S. *J. Phys. Chem.* **1993**, 97, 7147.

- (3) de Levie, R. In *Advances in Electrochemistry and Electrochemical Engineering*; Gerischer, H., Tobias, C. W., Eds.; Interscience: New York, 1984; Vol. 13, p 1.
- (4) Fan, F.-R. F.; Bard, A. J. *Science* **1995**, 267, 871.
- (5) Penner, R. M.; Heben, M. J.; Longin, T. L.; Lewis, N. S. *Science* **1990**, 250, 1118.
- (6) Morris, R. B.; Franta, D. J.; White, H. S. *J. Phys. Chem.* **1987**, 91, 3559.
- (7) Pendley, B. P.; Abruña, H. D. *Anal. Chem.* **1990**, 62, 782.
- (8) Mirkin, M. V.; Fan, F.-R. F.; Bard, A. J. *Science* **1992**, 257, 364.
- (9) Wong, D. K. Y.; Xu, L. Y. F. *Anal. Chem.* **1995**, 67, 4086.
- (10) (a) Menon, V. P.; Martin, C. R. *Anal. Chem.* **1995**, 67, 1920. (b) Martin, C. R., private communication, 1995.
- (11) (a) Bond, A. M.; Oldham, K. B.; Zoski, C. G. *Anal. Chim. Acta* **1989**, 216, 177. (b) Oldham, K. B.; Zoski, C. G. *J. Electroanal. Chem.* **1988**, 256, 11.
- (12) (a) Baranski, A. S. *J. Electroanal. Chem.* **1991**, 307, 287. (b) Oldham, K. B. *Anal. Chem.* **1992**, 64, 646.

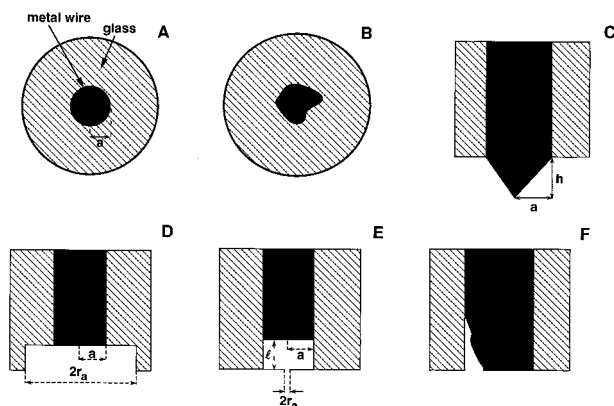


Figure 1. Different shapes of ultramicroelectrodes. (A) A perfect microdisk electrode. (B) An irregularly shaped disk-type planar UME. (C) A convex UME with a metal wire protruding from the glass sheath. (D) A recessed electrode with the circular hole in the insulating sheath larger than the conductive disk. (E) A "lagooned" electrode. (F) A leaky UME.

ments.<sup>1</sup> A tip with a conductor protruding from the insulating sheath (Figure 1C) may be shaped as a spherical cap or a cone. The former geometry can be produced by mercury deposition,<sup>13</sup> and conically shaped tips are usually made by etching.<sup>8,14</sup> Convex UMEs require thorough characterization and should be used cautiously.

If the tip is recessed into the glass insulator (Figure 1D,E), its voltammetric behavior depends on the relation between the radius of a conducting core and that of the aperture in the insulating sheath. When the opening in glass is significantly larger than the surface area of the metal exposed to solution (Figure 1D), the UME behavior may be not very different from that of the regular inlaid electrode. In contrast, Figure 1E represents the most dangerous "lagooned"<sup>12b</sup> geometry, i.e., an electrode with the metal recessed into the solution-filled microcavity inside the glass insulator. Such an electrode can mimic the behavior of a much smaller UME, and the measured apparent rate constant may be orders of magnitude higher than the true value.<sup>12</sup> A leaky UME (Figure 1F) can be easily identified from the relatively high double-layer charging current,  $i_c$ . The ratio of the  $i_c$  to the steady-state diffusion-limiting current is proportional to the sweep rate,  $v$ .<sup>1</sup> For a well-sealed submicrometer-sized UME, this ratio should be small even at sweep rates of the order of several volts per second. Significantly recessed and leaky electrodes should be identified and rejected.

It was shown previously<sup>15</sup> that the size and shape parameters of a small UME can be evaluated by using it as a tip electrode in the scanning electrochemical microscope (SECM; this abbreviation is also used for the method, i.e., microscopy<sup>16</sup>). In SECM, a redox mediator is either reduced or oxidized at the tip electrode. The product of this reaction diffuses to the substrate, where it

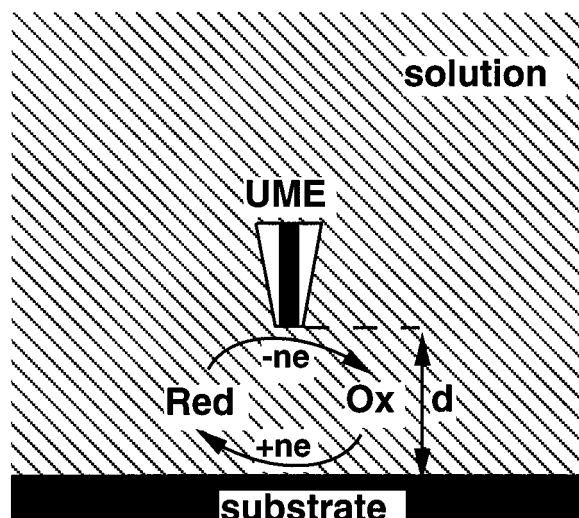


Figure 2. Feedback mode of SECM operation. The tip current increases as the tip approaches a conductive substrate due to the regeneration of the redox mediator. The shape of the tip current vs the tip–substrate distance curve depends on the tip geometry.

may be re-oxidized or re-reduced (Figure 2). This process produces an enhancement in the faradaic current at the tip electrode depending on the tip shape and the tip–substrate separation (positive feedback). When the tip is planar (Figure 1A,B), its entire surface is facing the substrate, and the distance,  $d$ , is the same for every point of the tip surface. If the tip is convex, e.g., conically shaped (Figure 1C), its sharp top prevents the substrate from approaching the main part of the tip surface.<sup>15</sup> The surface of a lagooned tip (Figure 1E) is screened from the substrate by the insulator. Thus, the feedback current for convex and recessed UMEs is significantly smaller than that for planar tips. The combination of the analysis of current–distance curves with SEM and voltammetry is used below to demonstrate that our submicrometer tips are planar or convex (depending on preparation) rather than recessed or leaky and, therefore, are suitable for quantitative measurements.

## EXPERIMENTAL SECTION

**Chemicals.** Hexaammineruthenium(III) chloride (99%, Strem Chemicals, Newburyport, MA), Nafion (5 wt %, Aldrich Chemical Co., Milwaukee, WI), chlorotrimethylsilane (Hüls America Inc., Bristol, PA), and all other chemicals were used as received. All solutions were prepared with deionized water (Milli-Q, Millipore Corp., Bedford, MA).

**Apparatus.** A BAS 100B electrochemical analyzer (Bioanalytical Systems, West Lafayette, IN) was used to perform cyclic voltammetric and film deposition experiments. A 1-mm-diameter BAS Pt electrode and indium tin oxide (ITO) on glass (Delta Technologies, Inc., Stillwater, MN) were used as the substrates. The same brand of ITO glass was previously employed as a SECM substrate,<sup>8</sup> characterized by AFM, and appeared to be smooth on the nanometer scale. The SECM apparatus was similar to that described previously<sup>17</sup> except for a CE-6000 controller (Burleigh Instruments, Inc., Fishers, NY) used to control three inchworm motors and a newer version of software generously provided by Prof. David O. Wipf (Mississippi State University). A four-electrode potentiostat (EI-400, Ensman Instruments, Bloomington,

(13) (a) Wehmeyer, K. R.; Wightman, R. M. *Anal. Chem.* **1985**, *57*, 1989. (b) Stojek, Z.; Osteryoung, J. *Anal. Chem.* **1989**, *61*, 1305.

(14) (a) Besenhard, J. O.; Schulte, A.; Schur, K.; Jannakoudakis, P. D. In *Microelectrodes: Theory and Applications*; Montenegro, M. I., Queirós, M. A., Daschbach, J. L., Eds.; Kluwer Academic Publishers: Dordrecht, 1991; p 189. (b) Zhang, X.; Zhang, W.; Zhou, X.; Ogorevc, B. *Anal. Chem.* **1996**, *68*, 3338.

(15) Mirkin, M. V.; Fan, F.-R. F.; Bard, A. J. *J. Electroanal. Chem.* **1992**, *328*, 47.

(16) For a review of the SECM, see: Bard, A. J.; Fan, F.-R. F.; Mirkin, M. V. In *Electroanalytical Chemistry*; Bard, A. J., Ed.; Marcel Dekker: New York, 1994; Vol. 18, p 243.

(17) Wipf, D. O.; Bard, A. J. *J. Electrochem. Soc.* **1991**, *138*, 469.

IN) was used for independent control of the tip and substrate potentials. A PAR Model 273 potentiostat (Princeton Applied Research, Princeton, NJ) and an IPZ-150M low-voltage piezo driver (Burleigh) served as voltage source for a PZL pusher (Burleigh). Potentiometric experiments were performed with a Fisher Accumet pH meter.

**Tip Preparation.** The tip preparation procedure involved pulling metal wires into glass pipets with the help of a P-2000 laser pipet puller (Sutter Instrument Co., Novato, CA). Platinum and silver microwires (50- $\mu\text{m}$  diameter) and borosilicate tubes (1.2-mm outer diameter, Sutter) were used as starting materials. Several different parameters of the pulling program can be varied in order to control the shape and size of the micropipet, e.g., the temperature of heating and the strength of pulling. In this way, one can change both radii of the metal and surrounding glass. A more detailed description of the pulling procedure can be found elsewhere.<sup>18</sup> Immediately after pulling, the metal core is entirely covered with glass, and the next step is to expose the tip of the wire. This can be done either by etching away a small portion of glass with 40% HF or by micropolishing. (**Caution:** 40% HF can cause severe lesions! Care should be taken to avoid skin contact.) The latter procedure was carried out using a BV-10 micropipet beveler (Sutter) equipped with a micromanipulator and a long working distance stereomicroscope. The micromanipulator was used to move the pipet toward the slowly rotating abrasive disk covered with 0.05- $\mu\text{m}$  alumina (Sutter). Initially, the axis of the pipet is perpendicular to the plane of the disk. When the pipet touches the disk, the small change in the angle can be detected microscopically. The size of the prepared tip increases with the length of etching or polishing. Only a fraction of the complete turn of the polishing wheel is required to produce a nanometer-sized polished electrode.

The electrode resistance was used to estimate the surface area of the electrode during preparation. When the tip is completely covered with glass, the resistance is extremely high, and it decreases sharply when the tip becomes exposed to solution either by etching or polishing. The tip resistance was monitored during either procedure. The impedance measurements can be carried out continuously either in the etching solution or in the polishing fluid. However, it seems preferable to measure resistance between the tip and the InGa alloy liquid at room temperature. Such an alloy does not wet glass and thus does not fill small pores in the insulating sheath. Thus, the sharp decrease in resistance results from exposure of the tip to solution rather than the appearance of a solution-filled cavity inside the glass sheath. The traces of InGa alloy and polishing materials were removed by washing the tips with concentrated HCl and acetone. In this way, electrodes with an effective radius as small as 2 nm (from voltammetry) and as large as a few micrometers can be manufactured. The geometries of UMEs prepared by etching and polishing turned out to be significantly different.

Ion-selective electrodes (ISEs) for silver and iodide were fabricated by coating etched Ag electrodes with AgI. The AgI coating was formed by electrolysis of 0.01 M KI + 0.1 M KNO<sub>3</sub> aqueous solution. While the thickness of the AgI film on larger silver electrodes (e.g.,  $a \geq 5 \mu\text{m}$ ) can be easily controlled using the BAS-100B potentiostat in its bulk electrolysis mode, the charge required for deposition of nanometer-thick AgI onto a sub-

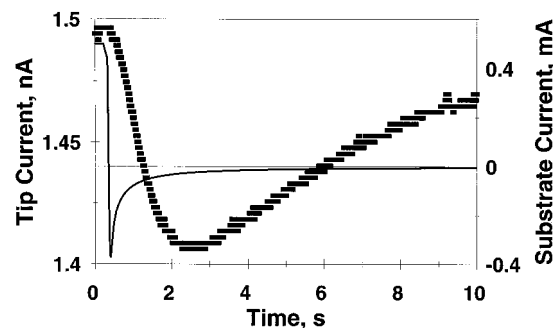


Figure 3. Time-of-flight experiment with the SECM. The tip (squares) and substrate (solid line) current transients were obtained by application of a 0.3-s potential pulse of  $-0.6 \text{ V}$  magnitude to the HOPG substrate. The tip was biased at  $-400 \text{ mV}$  vs Ag/AgCl reference. The distance between the 140-nm-diameter polished Pt tip and the substrate was  $106 \mu\text{m}$ . Solution was 10 mM in  $\text{Ru}(\text{NH}_3)_6^{3+}$  and 1 M in KCl. Initially, the substrate potential was 0 V.

micrometer-radius tip was too small to be controlled quantitatively. The Ag electrode was soaked in the iodide solution for 10 min, and the AgI coating was applied by running several cyclic voltammograms between  $+0.3$  and  $-0.6 \text{ V}$  vs Ag/AgCl. The Ag/AgI tips were coated with Nafion using a procedure similar to that described in ref 19. To improve the adhesion of Nafion film, the surface of the glass was silanized by application of several drops of chlorotrimethylsilane solution and subsequent drying in the air for 10 min.

**SECM Procedure.** To characterize submicrometer-sized electrodes by SECM, one needs to bring the tip into close proximity to a substrate surface.<sup>15</sup> A tip-substrate separation smaller than the tip radius,  $a$ , is required in order to obtain reliable information about the UME geometry. This is not a problem when the tip is micrometer-sized. However, positioning a very fragile nanometer-sized tip within a few nanometers distance from the substrate is challenging. Moving the tip toward the substrate at a scan rate faster than  $\sim 1 \text{ nm/s}$  leads to the tip crash. With an initial tip-substrate separation of a few millimeters, it would take an impractically long time to approach the substrate at a suitable scan rate. We employed SECM time-of-flight measurements<sup>20</sup> to determine the tip-substrate distance and reduce the approach time. A short pulse (from 0 to  $-0.6 \text{ V}$  vs Ag/AgCl) was applied to the substrate to produce a diffusion-controlled reduction of the mediator,  $\text{Ru}(\text{NH}_3)_6^{3+}$ . This caused a depletion of  $\text{Ru}(\text{NH}_3)_6^{3+}$  species in the gap and a decrease in the tip current (the tip potential was  $-0.4 \text{ V}$  vs Ag/AgCl). The obtained tip current transients exhibited a minimum point (Figure 3). The time corresponding to the minimum tip current is<sup>20b</sup>

$$t_{\min} = 0.11d^2/D \quad (2)$$

where  $d$  is the distance between the tip and the substrate and  $D$  is the diffusion coefficient of the mediator. With the known value of  $D$  ( $6.3 \times 10^{-6} \text{ cm}^2/\text{s}$  for  $\text{Ru}(\text{NH}_3)_6^{3+}$  1a), one can use eq 2 to evaluate the tip-substrate separation from the experimentally found  $t_{\min}$ . To check the correctness of the found  $d$  value, one can move the tip by several micrometers toward the substrate,

(19) Garguilo, M. G.; Michael, A. C. *Anal. Chem.* **1994**, *66*, 2621.

(20) (a) Feldman, B. J.; Feldberg, S. W.; Murray R. W. *J. Phys. Chem.* **1987**, *91*, 6558. (b) Mirkin, M. V.; Arca, M.; Bard, A. J. *J. Phys. Chem.* **1993**, *97*, 10790.

(18) Fish, G.; Bouevitch, O.; Kokotov, S.; Lieberman, K.; Palanker, D.; Turovets, I.; Lewis, A. *Rev. Sci. Instrum.* **1995**, *66*(5), 3300.

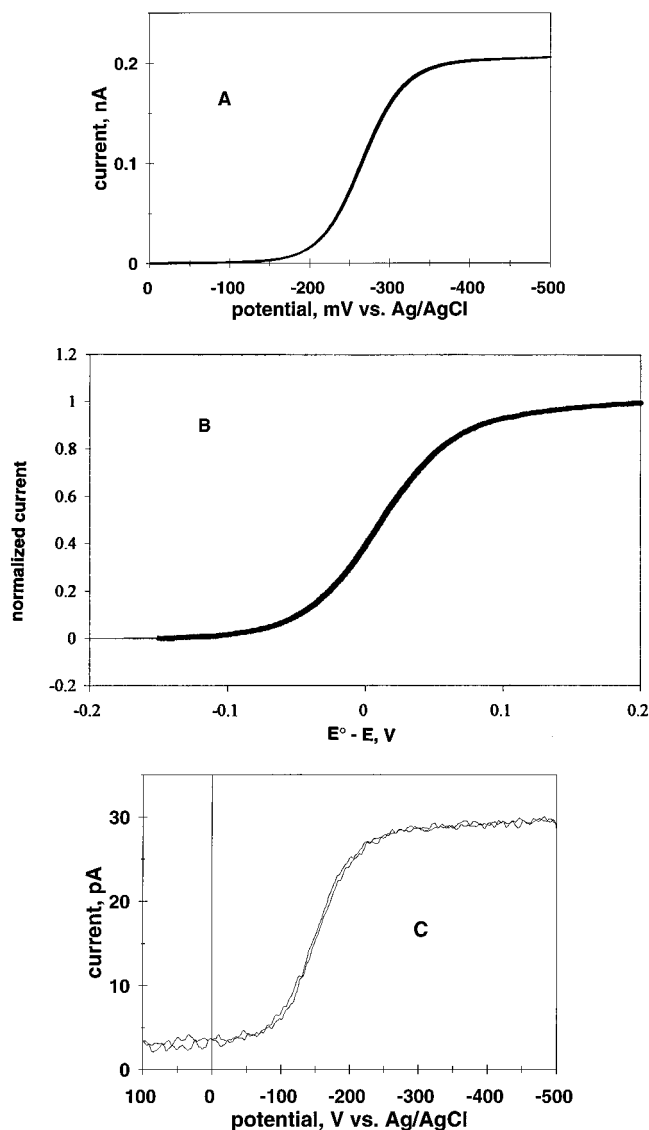


Figure 4. Steady-state voltammograms of  $\text{Ru}(\text{NH}_3)_6\text{Cl}_3$  at polished Pt electrodes. Solution contained (A) 10 mM  $\text{Ru}(\text{NH}_3)_6\text{Cl}_3$  and 1 M KCl; (B) 10 mM  $\text{Ru}(\text{NH}_3)_6\text{Cl}_3$  and 0.5 M  $\text{KNO}_3$ ; and (C) 50 mM  $\text{Ru}(\text{NH}_3)_6\text{Cl}_3$  and 0.5 M KCl. The effective electrode radius (assuming disk geometry) and the potential sweep rate were (A)  $a = 84$  nm,  $v = 20$  mV/s; (B)  $a = 22$  nm,  $v = 5$  mV/s; and (C)  $a = 2$  nm,  $v = 20$  mV/s. The thin line in (B) is the theory for a 22-nm microdisk.

measure another  $t_{\text{min}}$ , and calculate the new  $d$  from eq 2. The difference between the two distance values should be close to the actual piezo displacement.

Equation 2 should be applicable to a tip of any size as long as it is much smaller than the substrate. We tested this by using different tips, from 70-nm to 12.5- $\mu\text{m}$  radius. In all cases, the  $d$  values calculated using eq 2 were in agreement with those found from the piezo position. This methodology allowed us to quickly position a small tip within about 1- $\mu\text{m}$  distance from the substrate. After that, the tip was moved at a scan rate of a few angstroms per second using a piezoelectric pusher.

## RESULTS AND DISCUSSION

**Voltammetry.** Steady-state voltammetry can provide an estimate of the radius and demonstrate that the electrode response follows the theory. Figure 4A shows a steady-state voltammogram of 10 mM hexaammineruthenium(III) at a polished Pt electrode

whose effective radius appears to be 84 nm. At a scan rate of 20 mV/s, the voltammogram is very well shaped with a flat plateau and no detectable contribution from double-layer charging current. At a higher scan rate, e.g., 2 V/s, no peaks characteristic for non-steady-state diffusion could be detected, and the limiting current plateau remained flat. This indicates that the size of the electrode is significantly smaller than 1  $\mu\text{m}$ . A modest contribution of the charging current to the total current was consistent with the apparent radius of about 100 nm.

The response of a smaller tip ( $a = 22$  nm, thick line in Figure 4B) is in perfect agreement with the theory (thin line). The current at an even smaller ( $a \approx 2$  nm) electrode (Figure 4C) is slightly noisy. The voltammograms obtained at this electrode remained sigmoidal and retraceable at sweep rates as high as several volts per second. This indicates that the true area of the electrode is very small. In contrast, a "lagooned" electrode, whose true geometrical area is much larger than the effective area, should exhibit relatively high charging current and be slow to reach steady state.<sup>12</sup> Very low background currents observed at polished electrodes also indicate that there is no apparent solution leakage through the cracks in the glass insulator.

Unlike polished UMEs, voltammograms obtained at etched electrodes often exhibit larger background current and a considerable hysteresis. This can be expected if the metal wire protrudes significantly from the glass sheath, so that the UME is shaped as a sharp cone or a cylinder. These electrode geometries do not achieve perfect steady state. A large ratio of the surface area to the radius results in a significant charging current. Similar features in the voltammograms may, however, be caused by solution leakage or metal recession. To distinguish between these possibilities, we characterized several tips by SEM and SECM.

**Scanning Electron Microscopy (SEM).** A SEM micrograph of a relatively large polished Pt UME is shown in Figure 5A. One can clearly see a 1- $\mu\text{m}$ -radius ring of polished glass surrounding the  $\sim 150$ -nm-radius tip of the wire. Importantly, the metal is not recessed into the glass but slightly protrudes from it. This protrusion is quite small and should not significantly affect voltammetric characteristics of the tip. From the SEM micrograph of the 50-nm-radius tip (Figure 5B), one can see that the metal wire is close to the edge of the insulating glass. While this should not be very important for a voltammetric electrode, the use of such an UME as a SECM tip would require very precise tip-substrate alignment.

The tip in Figure 5B is the smallest polished UME that we could image with the SEM. The radius of the metal core for smaller electrodes can be evaluated only after etching away a significant (about 1  $\mu\text{m}$  long) portion of the glass sheath with hydrofluoric acid. The radius of the Pt wire in Figure 5C is about 30 nm, and its tip is too small to be seen under 30 000 $\times$  magnification ( $< 10$  nm). The micrographs of the etched electrodes (Figure 5D) showed no polished glass surrounding the metal wire that protrudes more significantly into the solution.

**Scanning Electrochemical Microscopy (SECM).** Our goal here is to distinguish between the planar and nonplanar tips. An approximate theory for SECM with convex (i.e., shaped as a cone or a spherical cap) tips was developed previously.<sup>15</sup> The responses of "lagooned" tips (Figure 1E) can be modeled using the approach of Smythe,<sup>21</sup> which was further developed by Amatore et al.<sup>22</sup> (see Supporting Information). The diffusion-limiting current to a

(21) Smythe, W. R. *J. Appl. Phys.* **1953**, *24*, 70.



Figure 5. Scanning electron micrographs of submicrometer-sized tips. Top to bottom: (A) 150-nm-radius polished Pt UME; (B) 50-nm-radius conductive disk somewhat displaced toward the edge of the 1- $\mu\text{m}$ -radius glass ring; (C) Pt wire obtained by stripping  $\sim 1 \mu\text{m}$  of glass from the unpolished Pt UME; and (D) etched UME.

recessed microdisk with the orifice radius,  $r_a$ , significantly smaller than the disk radius,  $a$ , is

$$i_{T,\infty} = \frac{4nFDc^\circ r_a}{1 + (1.2/\pi)l/a} \quad (\text{S9})$$

where  $l$  is the depth of the metal recession (Figure 1E). The  $i_{T,\infty}$

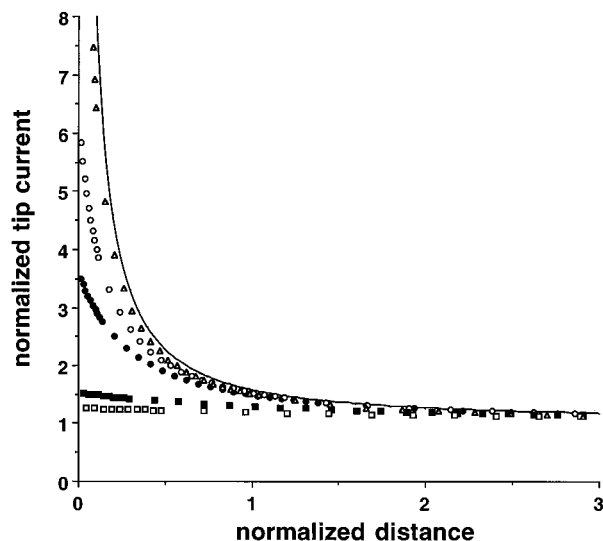


Figure 6. Steady-state current–distance curves for a “lagooned” tip over a planar conductive substrate corresponding to different values of the parameter  $l/a$  and the analogous working curve for a disk-shaped tip.  $l/a = 10$  ( $\square$ ), 5 ( $\blacksquare$ ), 1 ( $\bullet$ ), 0.5 ( $\circ$ ), and 0.1 ( $\triangle$ ). The upper curve was computed for a disk-shaped tip from eq S11.

computed from eq S9 is equal to the diffusion-limiting current at a regular inlaid microdisk of radius  $r = r_a/[1 + (1.2/\pi)l/a]$ . When a lagooned tip approaches a conductive substrate, the current–distance dependence is given by eq S12:

$$i_{\text{SECM}} = \frac{4nFDc^\circ r_a I_T}{1 + (1.2/\pi)I_T l/a} \quad (\text{S12})$$

and the corresponding normalized tip current,  $I_{\text{SECM}} = i_{\text{SECM}}/i_{T,\infty}$ , is

$$I_{\text{SECM}} = \frac{I_T[1 + (1.2/\pi)l/a]}{1 + (1.2/\pi)I_T l/a} \quad (3)$$

where  $I_T$  is the normalized current for an  $r_a$ -radius inlaid disk tip given by eq S11. The maximum normalized tip current ( $I_{\text{SECM,max}} = i_{\text{SECM,max}}/i_{T,\infty}$ ) is observed when the substrate contacts the insulating sheath and plugs the orifice. From eq S13, one obtains

$$I_{\text{SECM,max}} = \frac{1 + (1.2/\pi)l/a}{(1.2/\pi)l/a} = 1 + \frac{\pi a}{1.2l} \quad (4)$$

A family of approach curves ( $I_{\text{SECM}}$  vs  $d/r_a$ ) calculated for different  $l/a$  values is shown in Figure 6. Clearly, the deeply recessed tips, i.e.,  $l \gg a$ , do not show any significant positive feedback and thus can be easily distinguished from nonrecessed electrodes. For example, the maximum normalized feedback current ( $I_{\text{SECM,max}}$ ) of only 1.26 can be found from eq 4 for  $l/a = 10$ . Comparison with the current–distance curve calculated for an equivalent inlaid disk (solid curve in Figure 6) shows that one can detect the lagooned geometry as long as the recess is not very small,  $l \gtrsim 0.5a$ . For smaller  $l$ , the approach curve analysis is problematic because it is not easy to obtain normalized feedback current higher than 3 or 4 using a small tip of any shape. There is, however, another important difference between the approach curves obtained with a regular and a lagooned tip: when an inlaid

(22) Amatore, C.; Savéant, J. M.; Tessier, D. J. *J. Electroanal. Chem.* **1983**, *147*, 39.

UME gets to within nanometer distance of the conductive substrate, a sharp increase in current takes place due to the onset of tunneling. In contrast, no tunneling may occur between the lagooned tip and the substrate without irreversible breaking of insulating glass unless the depth of the cavity ( $l$ ) and the glass wall thickness together is less than about 10 nm. This diagnostic criterion also allows one to distinguish between the recessed and protruding tips, whose current–distance curves are otherwise quite similar.<sup>8,15</sup>

Fan et al.<sup>23</sup> simulated a special case of a recessed electrode with the radius of the circular hole in the insulator equal to the disk radius. They also derived an approximate expression for a recessed tip with  $r_a = a$  similar to eq S9 (the only difference is in the factor of 4 instead of 1.2 in the denominator of eq S9). The response of such an UME (as well as the responses of ones with orifice larger than the conductive disk radius, Figure 1D) is controlled by the size of the conductive core rather than the orifice. If  $l < a$ , the voltammetric behavior of a recessed UME should be very similar to that of the inlaid one. Only a large recess may cause significant errors if such an electrode is employed in kinetic measurements. If  $r_a > a$ , the behavior of a recessed UME with the same  $l$  should be even closer to that of a normal, nonrecessed tip. This type of geometry can be diagnosed from the lack of a significant positive SECM feedback (large  $l/a$ ) or the absence of tunneling (smaller  $l/a$ ) until the breakage of the glass insulator.

A SECM current–distance curve for a polished Pt tip approaching Pt substrate is shown in Figure 7A. Good agreement between the experimental data (symbols) and the theoretical current–distance curve (solid line) for a microdisk electrode and a relatively large maximum value of the normalized tip current ( $I_{\text{SECM,max}} \approx 4$ ) suggest that the tip is a planar electrode with an effective radius of about 380 nm. It is very improbable that such an approach curve can be obtained with a lagooned electrode. Not only should the depth of the recession be much smaller than the disk radius, but the plane of the orifice has to be located exactly at the top of the glass insulator and be exactly parallel to the plane of the substrate. Similarly, no significant feedback current can be expected in the case of substantial solution leakage (Figure 1F). These observations, in combination with the above voltammetric and SEM results, indicate that the tip used in generating the data for in Figure 7A is an essentially planar electrode.

A current–distance curve obtained with an etched electrode (Figure 7B) is totally different. The feedback current now is much smaller, and the experimental data fit well the theory for a sharp 20-nm-radius conical tip with a height-to-radius ratio of 2.5. The same approach curve could fit the theory for a recessed electrode (Figure 6). The difference is in the onset of tunneling current observed at the tip–substrate distance of a few nanometers. After the tip current increased sharply, the tip was retracted, and the  $I_{T,\infty}$  (the current to the tip far from the substrate) remained essentially unchanged. This means that the tunneling occurred without breaking the insulating glass, which would not be possible with the metal recessed into the glass insulator.

**Measurements of Heterogeneous Kinetics.** Another way to check the response of small UMEs is to measure the rate of a well-characterized rapid heterogeneous electron transfer. One such reaction is a one-electron reduction of  $\text{Ru}(\text{NH}_3)_6^{3+}$  in chloride

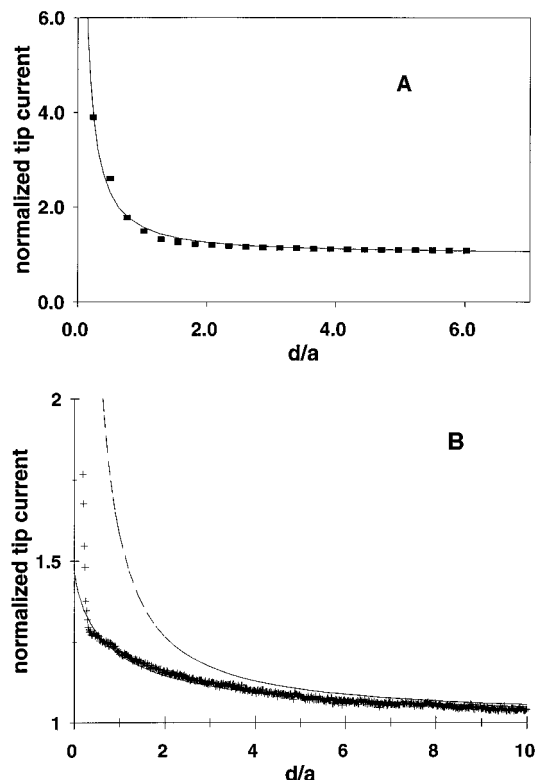


Figure 7. SECM current–distance curves obtained with a polished (A) and etched (B) submicrometer-sized tips. The conductive substrate was (A) polished Pt disk or (B) ITO glass. Thin lines show theoretical curves computed for (A) disk-shaped 380-nm-radius tip and (B) conical 20-nm-radius tip with the height-to-radius ratio of 2.5. The upper dashed curve in (B) represents the theory for a disk-shaped tip.

solution. Beriet and Pletcher recently studied this reaction by steady-state and fast-scan voltammetry at micrometer-sized (i.e., 1.1–12.5- $\mu\text{m}$  radius) Pt electrodes.<sup>24</sup> All steady-state voltammograms in ref 24 were Nernstian, giving a lower limit for the rate constant of about 0.7 cm/s. The  $k^0$  values from fast-scan cyclic voltammograms were close to 0.9 cm/s. This value is only slightly higher than that measured by Wipf et al.<sup>25</sup> in a trifluoroacetate solution ( $k^0 = 0.45$  cm/s). In contrast, Penner et al.<sup>5</sup> found that the rate of reduction of hexaammineruthenium(III) increases markedly in chloride medium. From steady-state voltammetry at a 203- $\text{\AA}$  electrode, they found  $k^0 > 11$  cm/s in 0.5 M KCl. The value of  $k^0 = 79 \pm 44$  cm/s for this reaction was measured at an 11- $\text{\AA}$  UME.<sup>5</sup> The origin of the discrepancy between the rates measured at nanometer- and micrometer-sized UMEs remains unclear. Besides the possibility of uncompensated resistive drop at larger electrodes<sup>5</sup> and shape uncertainties inherent for nanodes,<sup>12</sup> one cannot exclude special effects, e.g., film formation, which may have more influence on voltammograms at larger UMEs.<sup>26</sup>

We used the previously developed procedure<sup>27</sup> to extract the rate constant values from steady-state voltammograms of 10 mM  $\text{Ru}(\text{NH}_3)_6^{3+}$  obtained at different size UMEs (Table 1). Two different tables of rate constants were presented in ref 27, one

(24) Beriet, C.; Pletcher, D. *J. Electroanal. Chem.* **1994**, *375*, 213.

(25) Wipf, D. O.; Kristensen, E. W.; Deakin, M. R.; Wightman, R. M. *Anal. Chem.* **1988**, *60*, 306.

(26) Kamau, G. N.; Saccucci, T. M.; Gounili, G.; Nassar, A.-E. F.; Rusling, J. F. *Anal. Chem.* **1994**, *66*, 994.

(27) Mirkin, M. V.; Bard, A. J. *Anal. Chem.* **1992**, *64*, 2293.

(23) Fan, F.-R. F.; Kwak, J.; Bard, A. J. *J. Am. Chem. Soc.* **1996**, *118*, 9669.

Table 1. Apparent Heterogeneous Rate Constants of  $\text{Ru}(\text{NH}_3)_6^{3+}$  Reduction in Chloride Solutions at Different Size Electrodes

$i_{T,\infty}$ , pA	effective radius, nm	[KCl], M	$k^0$ , cm/s
1340	551	1	>1
664	273	1	$2.5 \pm 1$
205	84.2	1	>7
77.2	31.7	0.1	$1.8 \pm 1$
29.1	11.9	0.1	$10 \pm 5$
19.1	7.8	0.1	$7 \pm 5$

for a uniformly accessible electrode (e.g., a hemisphere) and another for a microdisk UME. Since it is not clear which is more appropriate for our electrodes, the uncertainties in Table 1 are sufficiently large to cover the range of rate constant values obtained with both assumptions. In spite of large uncertainties ( $k^0$  values are between 1.8 and 10 cm/s; see also the section on Limitations of Ultrasmall Electrodes below), one can see that there is no apparent correlation between the measured rate constant and the UME size. All rate constants in Table 1 are much lower than the value of 79 cm/s reported in ref 5, though the UMEs used were sufficiently small to exclude resistive effects. At the same time, our rate constants are significantly higher than those measured at larger electrodes. The  $k^0$  values obtained from fast-scan voltammetry may be underestimated because of the difficulties in resistance compensation and the use of the Nicholson method without accounting for nonlinear diffusion.<sup>28</sup>

**Potentiometric Tips.** The methodology described above allows one to make electrodes of different metals (e.g., Au, Pt, Ag, W, Ni). These can be used to produce potentiometric sensors, e.g., pH probes (Sb, W) and solid-state ISEs. The etched UMEs should be more suitable for preparation of submicrometer-sized potentiometric sensors because of their larger surface area. A 0.2- $\mu\text{m}$ -radius (from voltammetry) etched Ag tip coated with AgI showed stable linear responses to both  $\text{Ag}^+$  (Figure 8A; 56 mV/decade slope) and  $\text{I}^-$  (Figure 8B; -49 mV/decade slope) ions over the concentration range from  $10^{-5}$  to  $10^{-1}$  M. The ISE potential remained stable for hours.

Ultrasmall ISEs prepared by coated wire techniques may suffer from instabilities because of dissolution of the tiny amount of salt deposited on the surface. This problem can be overcome by application of a protective polymer film. Using a permselective polymer (e.g., Nafion), one can also eliminate some interferences. After the above Ag/AgI tip was coated with Nafion, its response to  $\text{Ag}^+$  (Figure 8C; 57 mV/decade slope) was very similar to that of an uncoated ISE except for a somewhat longer equilibration time, but the response to iodide vanished since Nafion film is impermeable for  $\text{I}^-$ . This indicated a nearly complete coverage of the tip by Nafion. The resistance of a relatively large (e.g., 0.2- $\mu\text{m}$  radius) electrode after coating remained sufficiently low to allow routine potentiometric measurements with a simple pH meter. However, more sophisticated equipment (e.g., a high-impedance electrometer) may be required for more resistive, nanometer-sized ISEs.

**Limitations of Ultrasmall Electrodes.** Several potential problems inherent in experiments with nanometer-size electrodes should be discussed. After one has proved the absence of detectable leakage of the insulating sheath and excluded the

possibility of the lagooned electrode, the geometry of a nanometer-sized tip remains incompletely known. This shortcoming is not equally important for different applications. For example, such an electrode can be used for analytical determinations as long as the diffusion-limiting current is proportional to the bulk concentration of the analyte. Both planar and convex tips are suitable for electrochemical imaging.<sup>16</sup> Geometric uncertainties should not be very important in the substrate generation/tip collection mode of SECM operation.<sup>16</sup> In this case, the tip travels within a thick diffusion layer generated by the substrate electrode, and the tip-substrate distance (averaged for different portions of the tip surface) is more important than the details of the UME geometry.

The effect of the UME shape on heterogeneous kinetics measurements is more complicated. Steady-state voltammetry seems to be the method of choice for nanometer-sized UMEs. Using the Shoup-Szabo equation,<sup>29</sup> one can see that the diffusion current to the microdisk approaches a steady-state value to within 10% at the time  $t \cong 10a^2/D$ . Assuming a typical value of  $D = 10^{-5}$  cm<sup>2</sup>/s, one obtains  $t \cong 2.5 \times 10^{-5}$  s for a 50-nm-radius UME. Thus, non-steady-state measurements with such an electrode should be carried on a microsecond time scale. This is not easy because the picoampere-range currents are to be measured. The shape uncertainties are also less important for steady-state than for transient measurements.<sup>11b,27</sup> When the electrode surface is uniformly accessible (e.g., a hemisphere or a rotating disk electrode), no information about its geometry is required for determination of kinetic parameters from steady-state voltammetry.<sup>27</sup> In contrast, if the electrode surface is not uniformly accessible (e.g., due to the edge effects), the rate constant values extracted from steady-state voltammograms depend significantly on tip geometry.<sup>11b,27</sup> Here, we are only interested in relatively fast processes for which  $k^0 \geq D/a$ , because for slower reactions one can use a larger electrode. The expected error range can be evaluated by comparison of  $k^0$  values which would be found from the steady-state voltammogram obtained at a nonuniform UME if the data were analyzed assuming the uniform accessibility of its surface. The theory for such calculation is available for a microdisk electrode. The comparison of the tables of kinetic parameters for a microdisk and a uniformly accessible electrode in ref 27 showed that the relative error for  $D/a \leq k^0 \leq 8D/a$  (the last value is close to the upper limit of  $k^0$  that can be determined reliably) is of the order of  $\pm 50\%$ . This value, though not very small, is still acceptable for fast kinetic measurements, where the results are often precise to within a factor of 2.

One can expect extremely small electrodes to obey macroscopic rules to only a certain extent. When the electrode size becomes comparable to that of electroactive molecules, the applicability of conventional diffusion equations is limited. A typical example is an unusual decrease in apparent electron transfer rate at higher concentrations of a supporting electrolyte recently observed with an array of nanometer-sized disks.<sup>10b</sup> Other deviations from conventional electrochemical theory at very small electrodes and in nanometer-thick thin-layer cells were predicted.<sup>30</sup> Since these effects are very hard to assess quantitatively, the size of the UMEs employed for kinetic experiments should be sufficiently large to avoid any of the microscopic effects described in ref 30. This corresponds to  $a \geq 10$  nm when a large excess of supporting electrolyte is present. With respect to the

(28) Lavagnini, I.; Pastore, P.; Magno, F. *J. Electroanal. Chem.* **1992**, *333*, 1.

(29) Shoup, D.; Szabo, A. *J. Electroanal. Chem.* **1982**, *140*, 237.

(30) Smith, C. P.; White, H. S. *Anal. Chem.* **1993**, *65*, 3343.

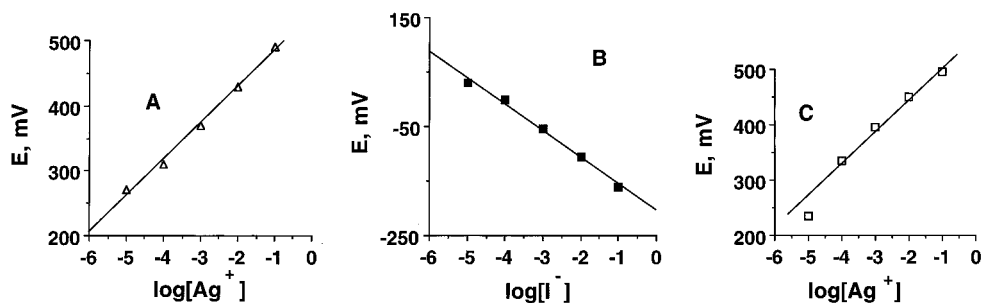


Figure 8. Calibration plots of potential against concentration of  $\text{Ag}^+$  (A and C) or  $\text{I}^-$  (B) for a  $0.2\text{-}\mu\text{m}$ -radius  $\text{Ag}/\text{AgI}$  tip in  $0.1\text{ M KNO}_3$ . The slope values (mV/decade) are (A) 56, (B)  $-49$ , and (C) 57.

feedback-mode SECM measurements with a conductive substrate, the ultimate lower limit for tip radius is about  $10\text{--}20\text{ nm}$ . This is because the most valuable kinetic information is contained in the portion of the current–distance curve where  $d \leq a$ . For smaller electrodes, the onset of the electron tunneling between tip and substrate at  $d \approx a$  would impair electrochemical measurements. This also complicates characterization of very small tips by SECM. Overall, quantitative measurements with ultrasmall UMEs are not straightforward. A significant percentage of the tips produced do not exhibit ideal behavior. Various irregularities have been observed. For instance, a very small surface of a voltammetric UME can easily be covered with impurities contained in solution because of the fast mass transport. Although this problem is less important for steady-state measurements, which are relatively insensitive to the adsorption, a slow decrease in tip current was sometimes observed. The use of pure chemicals and the avoidance of epoxy and other slightly soluble sealing and mounting materials is important for such experiments. The tip surface can often be regenerated by soaking the tip in acetone for a few hours.

## CONCLUSIONS

We have described two relatively simple procedures for preparation of nanometer-sized electrodes. The geometry of etched electrodes appears to be conical; they are suitable for preparation of ion-selective electrodes and biosensors. The micropolishing procedure leads to planar UMEs that exhibit well-behaved voltammetry and can be used as amperometric sensors. Both types of electrodes can serve as the SECM tips. The results of voltammetric, SEM, and SECM characterization of relatively large tips ( $a \geq 100\text{ nm}$ ) indicate that these electrodes are suitable for quantitative electrochemical measurements. Although sub-micrometer-sized UMEs cannot possess a perfect (e.g., disk)

geometry, one can still use them for kinetic experiments assuming uniform surface accessibility and using the effective value of the “superficial diameter”<sup>11b</sup> found from steady-state voltammograms. Such an assumption should not lead to excessively high errors and can be checked by measuring kinetic parameters for a well-characterized electron transfer reaction used as a reference.

Additional efforts are needed to ensure reliability of measurements with smaller (e.g., less than  $100\text{-nm}$  diameter) amperometric tips. One has to be cautious in interpreting the results to avoid artifacts. Nevertheless, such electrodes are very promising as a tool for electrochemical characterization of interfacial processes with nanometer-range resolution. The experiments aimed to further characterize nanometer-sized tips and improve their reproducibility are underway in our laboratories.

**Acknowledgment** is made to PSC–CUNY for the partial support of this research (M.V.M.). Our thanks are extended to David Wipf for providing the CE-6000 software package for data acquisition and for his assistance in building the SECM apparatus. We gratefully acknowledge the help of Fu-Ren Fan and Michael Tsionsky with early experiments and enlightening discussions with Allen Bard.

## SUPPORTING INFORMATION AVAILABLE

Theory of the SECM with a “lagooned” tip (2 pages). Ordering information is given on any current masthead page.

Received for review September 5, 1996. Accepted January 22, 1997.<sup>⊗</sup>

AC960887A

<sup>⊗</sup> Abstract published in *Advance ACS Abstracts*, March 1, 1997.